The Breakdown of de Gennes Scaling in $Tb_xEr_{1-x}Ni_2B_2C$ and Its Mean Field Theory Explanation

by

Chunwang Gao

A creative component submitted to the graduate faculty
in partial fulfillment of the requirements for the degree of
MASTER OF SCIENCE

Major: Condensed Matter Physics

Program of Study Committee:
Paul C. Canfield (Major Professor)
Harmon N. Bruce
Steven D. Kawaler
Ralph W. McCallum

Iowa State University
Ames, Iowa
2004

IST 2051

The Breakdown of de Gennes Scaling in $Tb_xEr_{1-x}Ni_2B_2C$ and Its Mean Field Theory Explanation

ABSTRACT

The Neel temperatures, T_N, of $Tb_xEr_{1-x}Ni_2B_2C$ samples have been determined from the temperature dependence of magnetization measurements. A breakdown of the de Gennes scaling of T_N with a clear turning point around x=0.45 has been observed. The T_N values of $Tb_xEr_{1-x}Ni_2B_2C$ do not change much within the range of $0<x<0.45$ and then, for larger x they increase almost linearly with concentration until T_N=14.9K is reached for x=1, $TbNi_2B_2C$. The clear change in the x-dependence of T_N around x=0.45 can be linked to a change in the local moment ordering direction from transverse to longitudinal, a change which is consistent with recent resonant X-ray scattering data. These features in $T_N(x)$ can be explained using a mean field model.

I. INTRODUCTION

RNi_2B_2C compounds attracted a lot of attention after their discovery in 1994 [1][2][3]. The structure of these compounds is I4/mmm tetragonal, with RC layers separated by Ni_2B_2 sheets. Low-temperature antiferromagnetic ordering is found in these compounds for several magnetic rare earth elements, including Gd ($T_N \approx 19.5$ K), Tb ($T_N \approx 14.9$ K), Dy ($T_N \approx 10.3$ K), Ho ($T_N \approx 6.0$ K), Er ($T_N \approx 6$ K), and Tm ($T_N \approx 1.5$ K) [4]. Superconductivity is also reported for both nonmagnetic elements, i.e. Lu ($T_C \approx 16.5$ K) and Y ($T_C \approx 15.7$ K), and magnetic elements, i.e. Tm ($T_C \approx 10.8$ K), Er ($T_C \approx 10.5$ K),

Ho ($T_C \approx 8.5$ K) and Dy ($T_C \approx 6.2$ K). Antiferromagnetic ordering temperatures (T_N) and superconductivity critical temperatures (Tc) generally follow de Gennes scaling as in Figure 1 [4].

$TbNi_2B_2C$ and $ErNi_2B_2C$ have many magnetic properties in common. Both compounds order antiferromagnetically with moments along the [100] direction. Both compounds have a magnetostriction-induced tetragonal-to-orthorhombic phase transition below T_N [5][6]. $ErNi_2B_2C$ becomes superconducting below $T_C \approx 10.5$ K, and orders antiferromagnetically below $T_N \approx 6$ K [7]. $TbNi_2B_2C$ does not become superconducting. It does have antiferromagnetic ordering below $T_N \approx 14.9$K [8]. Both compounds have an incommensurately modulated wave vector around (0.55, 0, 0) just below the T_N, however, $ErNi_2B_2C$ orders transversely [5] and $TbNi_2B_2C$ orders longitudinally [6]. A series of $Tb_xEr_{1-x}Ni_2B_2C$ compounds are studied in this paper so as to better understand the interaction and competition between the Er and Tb local moments and their ordered states.

II. EXPERIMENTAL METHODS

1. Flux Growth of Single Crystal of RNi_2B_2C

Samples of $Tb_xEr_{1-x}Ni_2B_2C$ were grown by a high-temperature flux growth technique using Ni_2B as solvent, a technique that was used to grow many other RNi_2B_2C single crystals. We choose Ni_2B as the solvent for several reasons. First, its melting point (≈1100°C) is well below the decomposition temperature of RNi_2B_2C (>1500°C). Second, both Ni and B are already included in the RNi_2B_2C, therefore, the solvent does not introduce new elements and thereby reduces the chance of impurities.

The growth process involves several steps. Polycrystalline NiB buttons are prepared using a large arc melter to reduce the loss of boron during arc melting. The NiB buttons are cut into pieces and used in preparation of RNi_2B_2C and Ni_2B starting material. Polycrystalline RNi_2B_2C buttons are prepared by arc meting a mixture of Ames Lab rare earth, high purity carbon and the pieces of NiB under argon gas on a water-cooled copper hearth. Ni_2B flux is prepared in a similar manner using a mixture of Ni and NiB cut into small pieces. The finger shaped ingot of RNi_2B_2C is then placed on the top of the equal mass of Ni_2B pieces inside a 5 ml alumina crucible. The crucible is hung inside a vertical tube furnace under flowing, high purity, and argon gas and heated according to the temperature and time profile shown in Figure 2. The purpose of the two-hour dwell at 200°C is to flush residual oxygen out of the system. The slow heating from 1450°C to 1480°C is done so as to let the Ni_2B dissolve as much of the RNi_2B_2C as possible and also to homogenize the mixture. The slow ramp to 1480 also helps to prevent overshooting the maximum temperature of the vertical tube furnace: 1500°C. There is then a slow cooling period from 1480°C to 1200°C over 80 hours, after which the furnace is shut down and cool to room temperature in about 12 hours. The 5 ml alumina growth crucible with everything inside is then sealed into a quartz tube with a partial pressure of argon gas and put into a furnace that is already stable at 1200°C. After two hours, the excess flux is separated from the crystals by a high-speed decant and plate-like crystals can be found at the bottom of the crucible. Crystal can be as big as 500mg in mass. The surface of the plate is normal to the crystalline c axis and the a, b axes as well as the [110] direction can be easily identified.

The samples of $Tb_xEr_{1-x}Ni_2B_2C$ are grown using the above procedure. Tb and Er are put in a molar ratio of x : (1-x) in the initial mixture. In order to establish the concentration of Tb:Er in the grown crystals, microprobe analysis was done on some of the samples. Table 1 is the summary of microprobe data, which show that the final ratio of Tb and Er is very close to the initial or nominal ratio.

2. Magnetization and Resistance Measurements

The temperature dependence of the static magnetization data was measured using a Quantum Design superconducting quantum interference device (SQUID). Using the temperature and field environment of the SQUID and a Linear Research Inc LR400 four-wire ac resistance bridge, the temperature dependence of the in-plane resistivity was also measured. Platinum wires 0.08 mm in diameter were attached to the surface of a crystal surface by Epotek H20E silver epoxy.

III. RESULTS AND DISCUSSION

1. The prediction of Neel Temperature of $Tb_xEr_{1-x}Ni_2B_2C$ by only considering RKKY interaction between rare earth ions.

Antiferromagnetic ordering temperatures (T_N) and superconductivity critical temperatures (T_C) generally follow de Gennes scaling as in Figure 1. [4]

Several $R_xR`_{1-x}Ni_2B_2C$ series has been studied. The results of T_N and T_C of $Ho_{1-x}Dy_xNi_2B_2C$ are reported by B. K. Cho el. al. [9] as shown in Figure 3. The Neel temperatures of the series follow the de Gennes scaling very well. The result is not surprising since the Ho and Dy moments inside the RNi_2B_2C crystals have a lot of

properties in common: they have similar saturated magnetic moments; they both have easy axis along [110] and they both have wave vector [001] at low temperature. The simple and understandable behavior of $T_N(x)$ for the $Ho_{1-x}Dy_xNi_2B_2C$ series lead to the question: what will $T_N(x)$ be for the $Tb_xEr_{1-x}Ni_2B_2C$ series?

$ErNi_2B_2C$ has $T_N \approx 6K$ [7] and Er ions order transversely just below T_N [5]. $TbNi_2B_2C$ has T_N 14.9K [8] and Tb ions order longitudinally just below T_N [6]. If we consider only the RKKY interaction between ions, the T_N of $Tb_xEr_{1-x}Ni_2B_2C$ should increase linearly with x, as showed by the dashed, green, straight line in figure 4.

In order to study how the antiferromagnetic ordering temperature, T_N, changes with concentration, the temperature dependent magnetization M(T) was measured for single crystals of $Tb_xEr_{1-x}Ni_2B_2C$ (x=0.0, 0.05, 0.1, 0.125, 0.15, 0.175, 0.2, 0.3, 0.4, 0.45, 0.5, 0.6, 0.8, and 1.0). M(T) data were collected by applying a magnetic field H=1000G for both H⊥c and H∥c direction, from which the polycrystalline average of $\chi(T)$ was calculated by $\chi_{poly}(T) = \frac{1}{3}\frac{M(T)_{H\parallel c}}{Hm} + \frac{2}{3}\frac{M(T)_{H\perp c}}{Hm}$ (m is the mass of the sample). Given that M. E. Fisher has shown [10] that $\frac{d(\chi T)}{dT} \propto c_p(T)$ for an antiferromagnetic material near Neel Temperature, T_N is defined as the temperature of the peak of the $\frac{d(\chi_{poly}T)}{dT}$ plot. The derivative is taken by averaging the slopes of two adjacent data points as follows: $\frac{1}{2}(\frac{y_{i+1}-y_i}{x_{i+1}-x_i} + \frac{y_i-y_{i-1}}{x_i-x_{i-1}})$. As a representative data set, $\chi_{poly}(T)$ data for $Tb_{0.20}Er_{0.80}Ni_2B_2C$ are plotted in Figure 5(a), and the $\frac{d(\chi T)}{dT}$ data for $Tb_{0.20}Er_{0.80}Ni_2B_2C$ are plotted in Figure 5(b). These data show that for the x=20% compound, T_N is 6.4K.

2. Discussion of the result

The experimental results of $T_N(x)$ over whole $Tb_xEr_{1-x}Ni_2B_2C$ series are shown in Figure 4. According to simple de Gennes scaling, the T_N values should follow a straight line from $ErNi_2B_2C$ to $TbNi_2B_2C$. These data display a clear breakdown of de Gennes Scaling. For comparison, two dotted straight lines (de Gennes Scaling) are drawn in the plot: the upper one is calculated by $T_N(x)_{\text{Simple dG}} = xT_{NTb} + (1-x)T_{NEr}$ and the lower one is calculated by using Gd ion's de Gennes factor and $GdNi_2B_2C$'s T_N, $T_{NGd} = 19.5K$ and assuming T_N is proportional to de Gennes factor of $Tb_xEr_{1-x}Ni_2B_2C$, $dG(x) = xdG_{Tb} + (1-x)dG_{Er}$. The experimental data show that instead of changing linearly, T_N changes very little for $x<0.4$, and then it increases almost linearly for $x>0.5$ until T_N=14.9K is reached. At the crossover point around x=0.45, the slope of the T_N changes suddenly giving rise to a sharp feature in $T_N(x)$.

The critical temperatures of superconductivity, T_C, are also shown in Figure 4. T_C is inferred from the temperature dependence of resistance of the samples. The data for $Tb_{0.1}Er_{0.9}Ni_2B_2C$ are plotted in Figure 6.

Figure 7 shows the difference between T_N estimated by simple de Gennes Scaling ($T_N(x)_{\text{Simple dG}} = xT_{NTb} + (1-x)T_{NEr}$) and the measured T_N. The peak in this difference is around x=0.45 and the shape of the data are almost symmetric on the two sides of the peak. The plot also clearly shows that there is a discontinuity around x=0.45.

The clear change in slope of the T_N in doping series indicates that something has changed around x=0.45, and our first guess is that at this point the direction of the ordered moments changes from transverse to longitudinal. For the pure compounds, $ErNi_2B_2C$ orders transversely and $TbNi_2B_2C$ orders longitudinally, therefore, if we

assume that the lightly doped samples order in the same manner, say, transversely or longitudinally, there should exist a critical concentration point at which the order direction switches and the switch could cause the slope of T_N to change suddenly. Resonant X-ray scattering experiments have been performed and the result show that this assumption is reasonable.

X-ray resonant scattering data on the series have been collected by C.Detlefs and the summary of his results are shown in table 2. Samples of 5 different concentration (x=0.125, 0.25, 0.5, 0.6 and 0.8) of Tb were measured and the T_N from x-ray data are consistent with M(T) measurement. τ is the modulation vector and it does not change significantly with x. In the Er rich compounds (x=0.125, 0.25), both Er and Tb moments are perpendicular to modulation vector after ordering, which means that for these x-values the Tb ions order transversely just like the Er ions do. In the Tb rich compounds (x=0.5, 0.6, 0.8), Tb ions order longitudinally like they do in pure $TbNi_2B_2C$. Unfortunately, the Er signal in Tb rich compounds was so small and it was no longer detectable. These results are consistent with our hypothesis that the sudden change in $T_N(x)$ is associated with a change from longitudinal to transverse order.

3. Mean Field Model

A mean field model can be set up based on both the magnetization data and X-ray data. Mean field theory assumes that any single ion experiences an average effective magnetic field from all other ions around it.

$$\vec{H}_{eff} = \frac{1}{g\mu_B} I < \vec{J}(\vec{R}) > . \qquad (1)$$

$< \vec{J}(\vec{R}) >$ is the average effect of other magnetic moments and I represents the interaction between magnetic moments. The Heisenberg Hamiltonian for a single ion without an external field will be:

$$H = g\mu_B \vec{J} \bullet \vec{H}_{eff} = I\{\vec{J} \bullet < \vec{J}(\vec{R}) >\} \qquad (2)$$

The anisotropy of the system is reflected by $I_{Transverse}$ and $I_{Longitudinal}$, which are two interaction terms for two different forms of order: transverse and longitudinal. $I_{Transverse} \neq I_{Longitudinal}$ means that there is an energy difference for the magnetic moments ordering transversely or longitudinally. Our assumption, which is consistent with X-ray data, is that in the doped compounds, Er ions and Tb ions will order in the same manner, either both transversely or both longitudinally. Because we can not know beforehand whether the ordering is transverse or longitudinal, in the fitting calculation for a certain I value and a certain temperature, we have to calculate the energy in both cases and the one with the lower energy will be used to determine the ordered direction. In the real calculation, we calculate two ordering temperatures, for transverse ordering and longitudinal ordering, and select the higher one to compare with the experimental data. There are four different I terms in our model to represent four different situations: $I_{ErTransverse}$ for Er moments order transversely, $I_{ErLongitudinal}$ for Er moments order longitudinally, $I_{TbTransverse}$ for Tb moments order transversely $I_{TbLongitudinal}$ for Tb moments order longitudinally.

Generally, The Neel temperature, T_N, will be proportional to $J(J+1) \cdot I$. Choosing the unit of the I terms so as to merge other factors into I terms, for pure $ErNi_2B_2C$ and $TbNi_2B_2C$, we have:

$$T_{N_{Er}} = \frac{1}{3} J_{Er}(J_{Er}+1) \cdot I_{ErTransverse}$$

$$T_{N_{Tb}} = \frac{1}{3} J_{Tb}(J_{Tb}+1) \cdot I_{TbLongitudinal}$$

The "$\frac{1}{3}$" is used to be consistent with other calculations.

For $Tb_xEr_{1-x}Ni_2B_2C$ compounds, two equations, which represent two ordering direction are used to fitting the data [11].

$$T_N^{Transverse} = \frac{1}{3}(1-x) J_{Er}(J_{Er}+1) \cdot I_{ErTransverse} + \frac{1}{3} x J_{Tb}(J_{Tb}+1) \cdot I_{TbTransverse}$$

$$T_N^{Longitudinal} = \frac{1}{3}(1-x) J_{Er}(J_{Er}+1) \cdot I_{ErLongitudinal} + \frac{1}{3} x J_{Tb}(J_{Tb}+1) \cdot I_{TbLongitudinal}$$

The fitting method is to first choose values of $I_{ErTransverse}$, $I_{ErLongitudinal}$, $I_{TbTransverse}$ and $I_{TbLongitudinal}$ and then calculate T_N for different concentration samples and compare the results with experimental data. We use T_N of $TbNi_2B_2C$ (x=1) and $ErNi_2B_2C$ (x=0) to calculate $I_{ErTransverse}$ and $I_{TbLongitudinal}$. The other two parameters, $I_{ErLongitudinal}$ and $I_{TbTransverse}$ are selected to fit the Neel temperatures of the doped samples. The fitting results are:

$$I_{ErTransverse} = 0.29K \qquad I_{ErLongitudinal} = 0.00K$$

$$I_{TbTransverse} = 0.48K \qquad I_{TbLongitudinal} = 1.07K$$

Figure 8 is the result of fitting to the model. The square points are the experimental data inferred from the M(T) measurements. The two lines are the fitting results for ordering transversely (smaller slope one) and longitudinally (larger slope one). Figure 8 shows that the model results agree well with the experimental data and clearly show the turning point of T_N near x=0.5.

4. Physical Significance of Interaction Terms

The interaction terms, I,come from the mean field model:

$$\vec{H}_{eff} = \frac{1}{g\mu_B} I < \vec{J}(\vec{R}) > . \qquad (1)$$

$$\mathrm{H} = g\mu_B \vec{J} \bullet \vec{H}_{eff} = I\{\vec{J} \bullet < \vec{J}(\vec{R}) >\} \qquad (2)$$

It is the difference between $I_{Transverse}$ and $I_{Longitudinal}$ that make the ions to order transversely or longitudinally. The RKKY interaction should play an improtant role in the ordering, just as in other RNi_2B_2C compounds. However, the RKKY interaction does not determine the direction between the ordered magnetic moments and the ordering wave vector and it will not cause $TbNi_2B_2C$ and $ErNi_2B_2C$ to order differently. There must be extra terms which will be different when the compounds order transversely or longitudinally.

$$I_{Transverse} = I_{RKKY} + I_{OtherTransverse}$$

$$I_{Longitudinal} = I_{RKKY} + I_{OtherLongitudinal}$$

For temperature just below the T_N, the mean field is small and we can do a expansion to represent the relationship between interaction term and the mean field.

$$I_{OtherTransverse} = A^T{}_0 + A^T{}_1 < \vec{J}(\vec{R}) > + A^T{}_2 < \vec{J}(\vec{R}) >^2 + \ldots$$

$$I_{OtherLongitudinal} = A^L{}_0 + A^L{}_1 < \vec{J}(\vec{R}) > + A^L{}_2 < \vec{J}(\vec{R}) >^2 + \ldots$$

The different between the two terms will be

$$\Delta I_{Other} = \Delta A_0 + \Delta A_1 < \vec{J}(\vec{R}) > + \Delta A_2 < \vec{J}(\vec{R}) >^2 + \ldots$$

$$\Delta A_i = A^T{}_i - A^L{}_i$$

It can be shown that if ΔA_0 is zero and the difference come from higher terms of $<\vec{J}(\vec{R})>$, the transition will be first order. Experiments [5][6] has clearly shown that the transition of $TbNi_2B_2C$ or $ErNi_2B_2C$ around T_N is a second order transition which require ΔA_0 to be non-zero, which means that the main part of the ΔI_{Other} is independent of $<\vec{J}(\vec{R})>$ and there is an energy different that is proportional to $<\vec{J}(\vec{R})>$.

The CEF (crystal electric field) effect plays an important roll in many properties of RNi_2B_2C compounds. It can make $I_{Transverse}$ different from $I_{Longitudinal}$ below T_N because of the magnetostriction-induced tetragonal-to-orthorhombic transition [5][6]. However, it can not be the dominant reason for transverse or longitudinal order within our model. The energy associated with the CEF effect will be proportional to the square of the mean field $<\vec{J}(\vec{R})>$. Such an energy difference will lead to a first order transition, as discussed above. We can understand this as follows: the lattice structure is tetragonal above T_N ($<\vec{J}(\vec{R})>=0$) and the CEF effect should not differentiate between the [100] and [010] directions. If CEF splitting is the reason for the compounds to order differently, the difference will have to come from the tetragonal to orthorhombic transition which happens below T_N and the corresponding I_{CEF} term has to be zero when $<\vec{J}(\vec{R})>$ is zero and not zero when $<\vec{J}(\vec{R})>$ is not zero. The above argument can apply to any effect that related to magnetostriction-induced tetragonal-to-orthorhombic transition such as magnetoelastic effect.

What we need is an energy term that is proportional to $<\vec{J}(\vec{R})>$. The classical dipole-dipole interaction [12] is a candidate and can give reasonable fittings for the pure $ErNi_2B_2C$ data. The classical dipole-dipole interaction alone cannot explain the pure

$TbNi_2B_2C$ data though. Jen Jensen believes [13] that anisotropy in RKKY interaction will contribute to interaction terms and make Tb moments order longitudinally. More work will need to be done to determine the real physics behind this proportional-to-$< \vec{J}(\vec{R}) >$ term.

IV. CONCLUSIONS

The experimental results of $T_N(x)$ over the whole $Tb_xEr_{1-x}Ni_2B_2C$ series display a clear breakdown of de Gennes Scaling. A mean field model can be set up to explain the $T_N(x)$ and the different ordering direction of $TbNi_2B_2C$ and $ErNi_2B_2C$. The model gives a good fitting with the experimental data. Calculations show that in the mean field model, CEF and magnetoelastic effects cannot be the main reason that causes TbNi2B2C and $ErNi_2B_2C$ order differently since the transition is a second-order transition. Classical dipole-dipole interaction has been used to fit the $ErNi_2B_2C$ data. More work needs to be done to find the physics behind the proportional-to-$< \vec{J}(\vec{R}) >$ energy term, which cannot be the CEF or magnetoelastic effect.

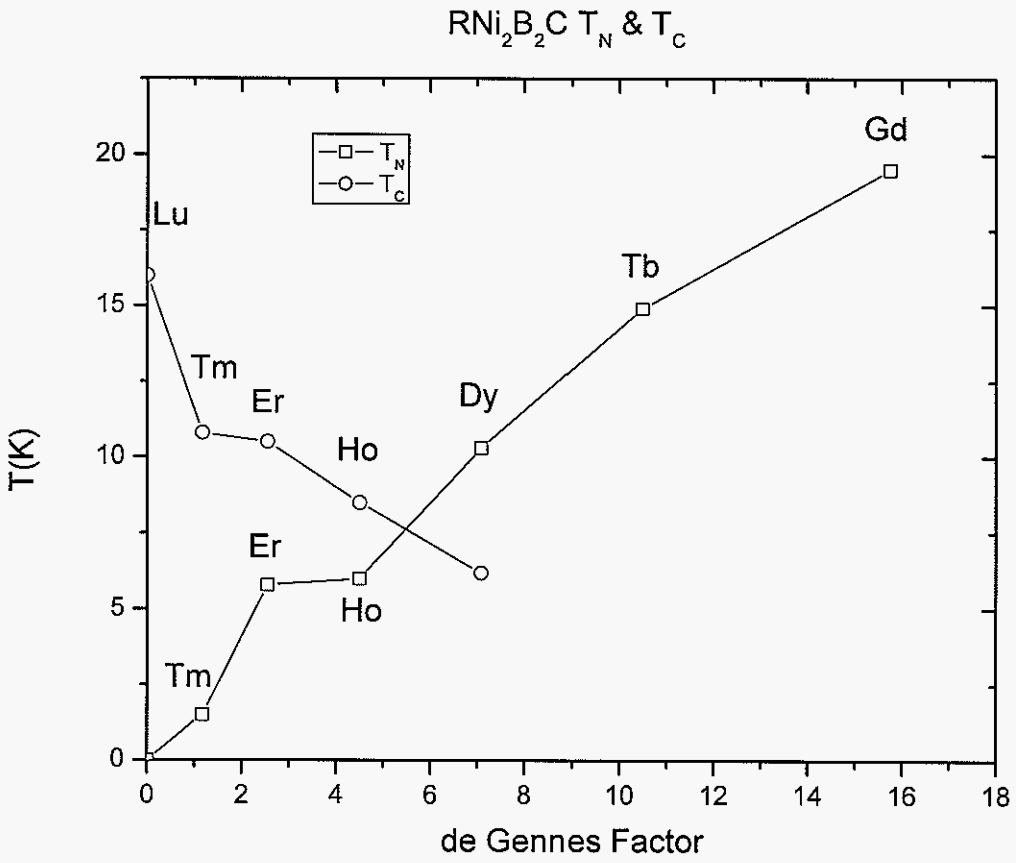

Figure 1. Neel Temperatures, T_N and Superconductivity Critical Temperatures, T_C of RNi_2B_2C. [4]

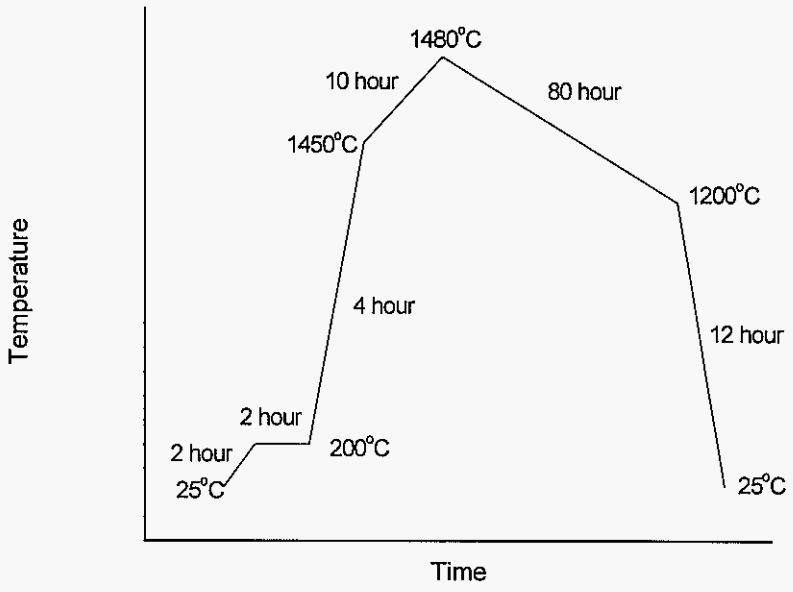

Figure 2. Temperature and time profile used in growth of $Tb_xEr_{1-x}Ni_2B_2C$

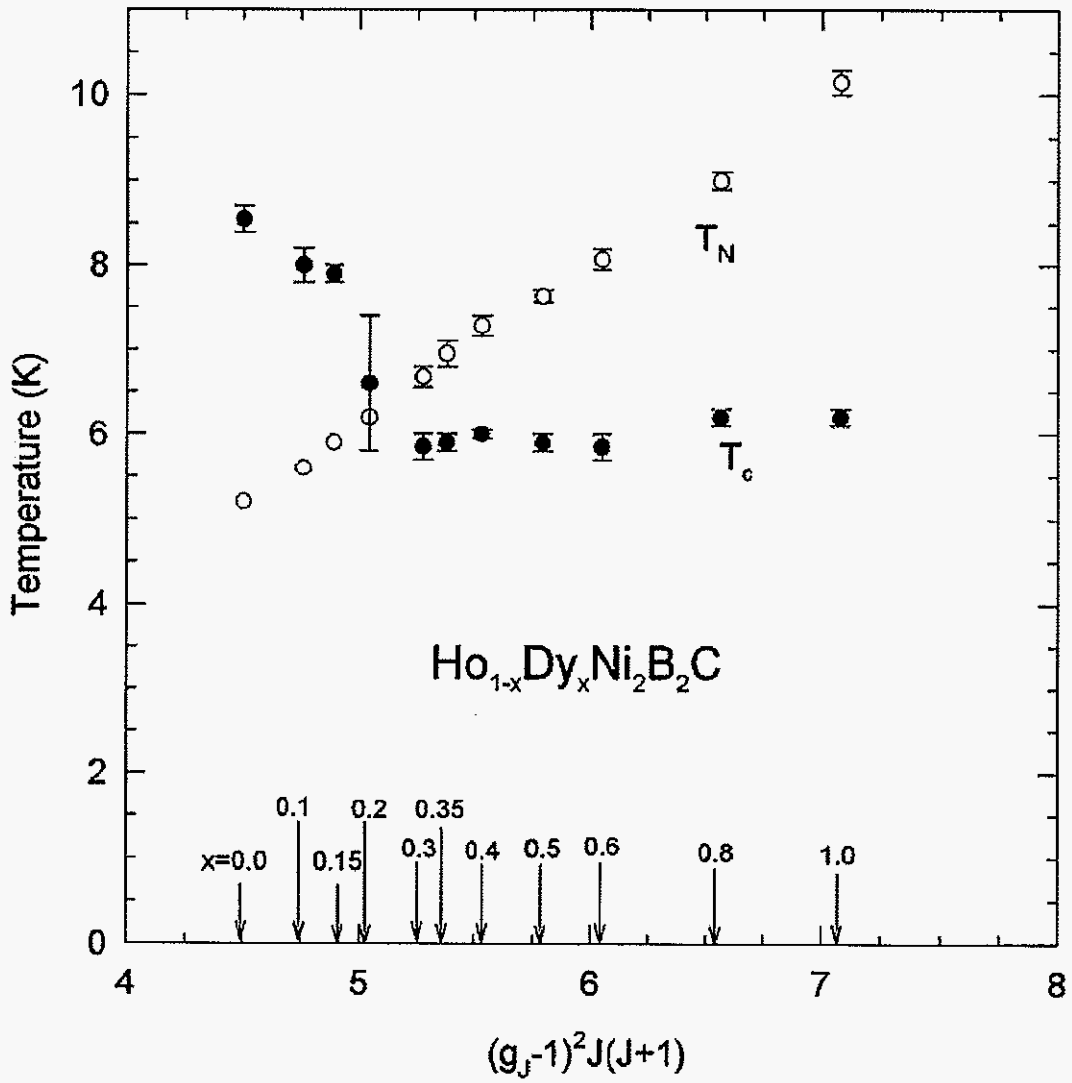

Figure 3. T_c and T_N vs dG factor for $(Ho_{1-x}Dy_x)Ni_2B_2C$. From reference [9], B. K. Cho, P. C. Canfield, and D. C. Johnston, Phys. Rev. Lett. 77, 163 (1996)

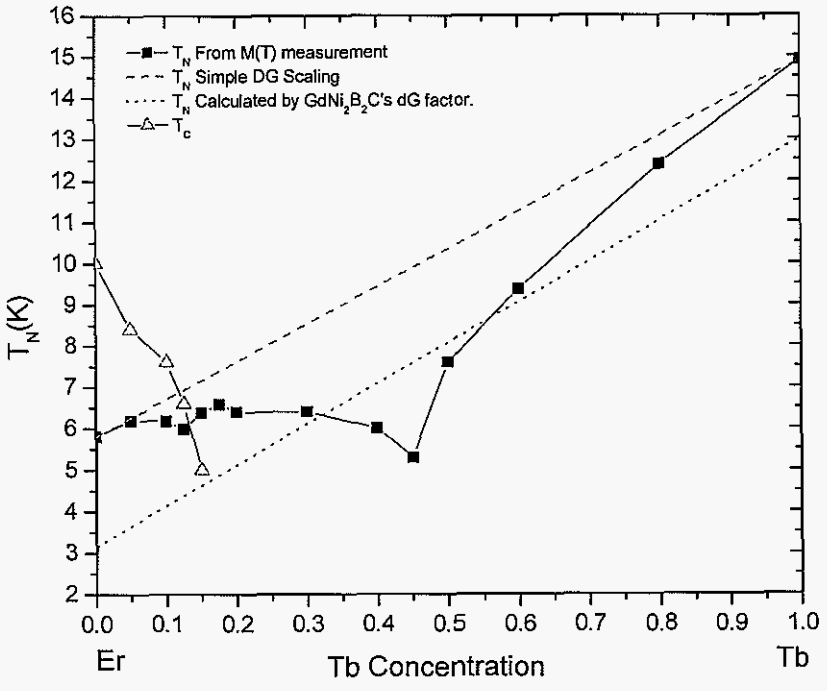

Figure 4. T_N and T_C of $Tb_xEr_{1-x}Ni2B2C$

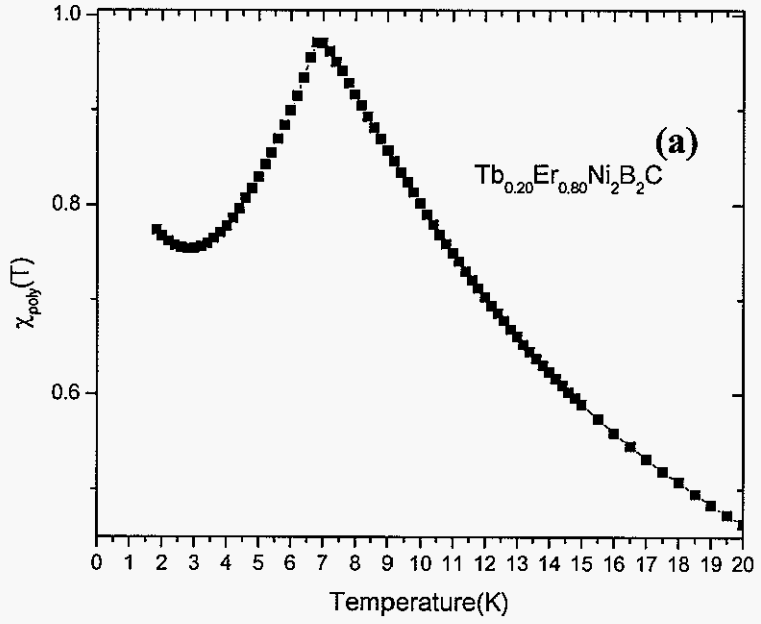

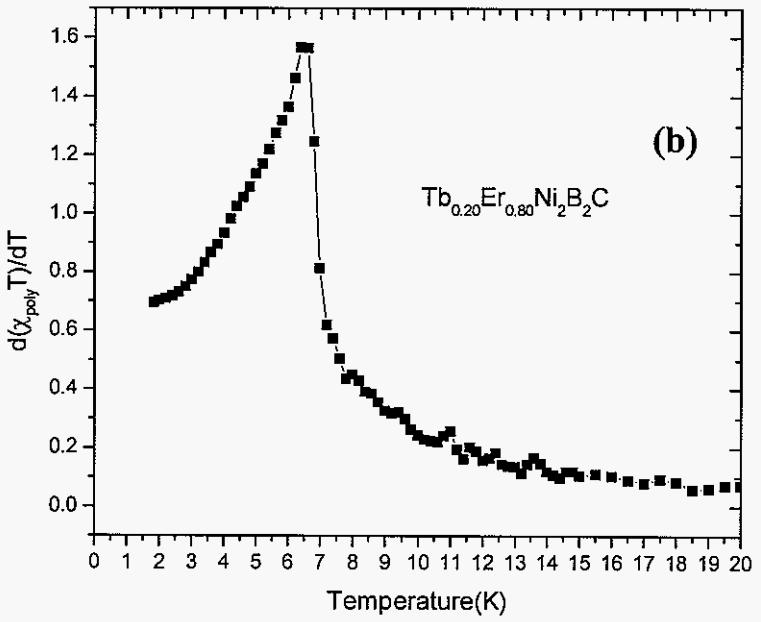

Figure 5. (a) $\chi_{poly}(T)$ and (b) $\frac{d(\chi_{poly}T)}{dT}$ data for $Tb_{0.20}Er_{0.80}Ni_2B_2C$

$\chi_{poly}(T) = \frac{1}{3}\frac{M(T)_{H\|c}}{Hm} + \frac{2}{3}\frac{M(T)_{H\perp c}}{Hm}$ The derivative is taken by averaging the slopes of two adjacent data points as follows: $\frac{1}{2}(\frac{y_{i+1}-y_i}{x_{i+1}-x_i} + \frac{y_i - y_{i-1}}{x_i - x_{i-1}})$

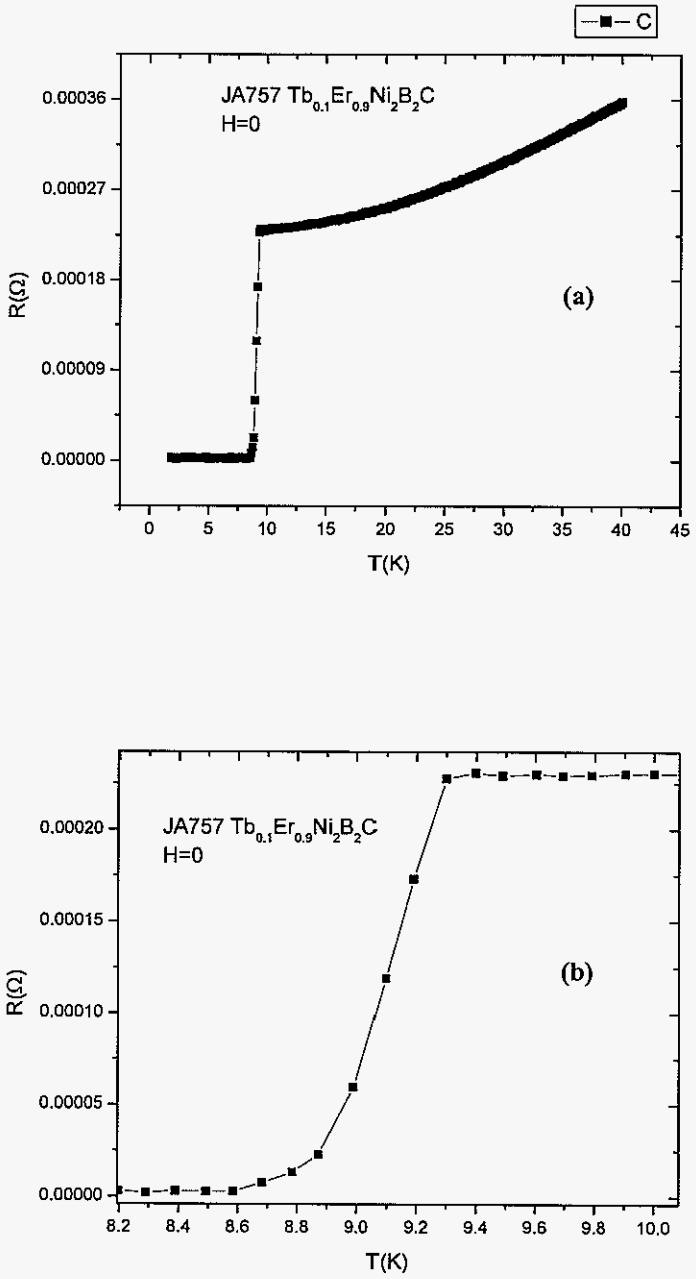

Figure 6. Temperature dependence of resistance for $Tb_{0.1}Er_{0.9}Ni_2B_2C$.

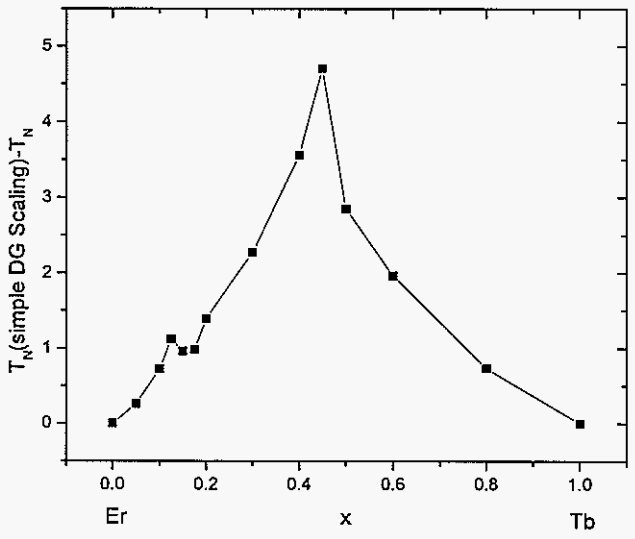

Figure 7. the difference between T_N estimated by simple de Gennes Scaling ($T_N(x)_{SimpledG} = xT_{NTb} + (1-x)T_{NEr}$) and the measured T_N.

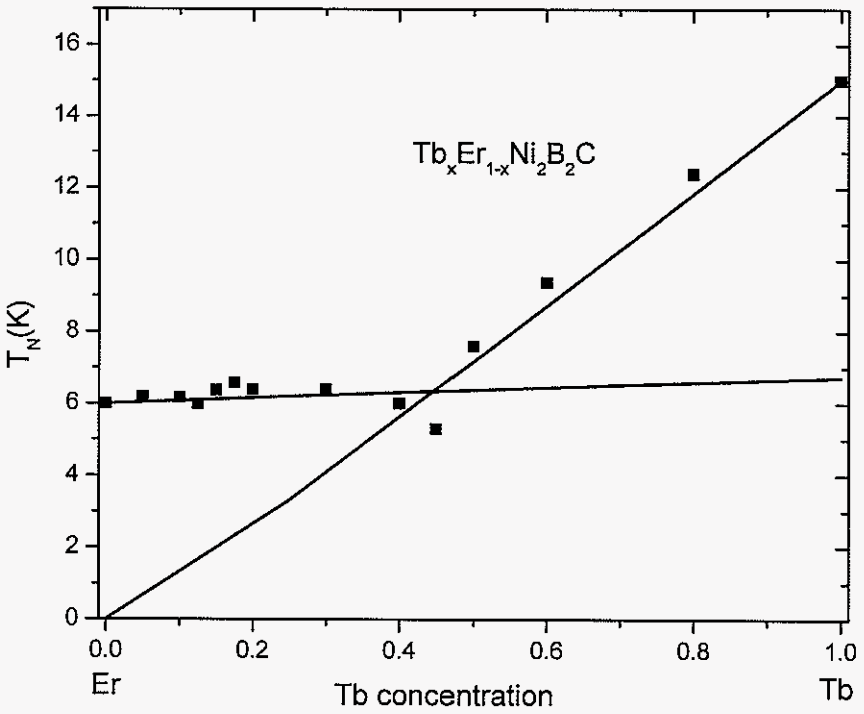

Figure 8. Fitting results of mean field model. The square points are the experimental data of T_N. The red line is the result of calculation for transverse ordering. The blue line is the result of calculation for longitudinal ordering.

Table 1. The microprobe result of the Tb:Er (mol ratio) compared with initial (nominal) ratio.

Initial ratio of Tb to Er as putting in (mol ratio)	Microprobe result of ratio of Tb to Er in $Tb_xEr_{1-x}Ni_2B_2C$ crystals. (mol ratio)
0.05:0.95	0.06:0.94
0.20:0.80	0.19:0.81
0.25:0.75	0.26:0.74
0.75:0.25	0.76:0.24
0.90:0.10	0.91:0.09

Table 2: Summary of x-ray resonant scattering results, x is the ratio of Er ions. $\parallel$ means magnetic moments are parallel to modulation vector (longitudinally). $\perp$ means magnetic moments are perpendicular to modulation vector (transversely)

Tb Concentration	T_N	T	μ_{Tb}	μ_{Er}
0.125	5.8	0.559	$\perp$	$\perp$
0.25	6.5	0.560	$\perp$	$\perp$
0.5	6.5	0.552	$\parallel$	
0.6	10	0.550	$\parallel$	
0.8	12	0.541	$\parallel$	

REFERENCES

[1] R. J. Cava, H. Takagi, H. W. Zandbergen, J. J. Krajewski, W. F. Peck, Jr., T. Siegrist, B. Batlogg, R. B. van Dover, R. J. Felder, K. Mizuhashi, J. O. Lee, H. Eisaki and S. Uchida, Nature (London) **367**, 252 (1994).

[2] R. Nagarajan, Chandan Mazumdar, Zakir Hossain, S. K. Dhar, K. V. Gopalakrishnan, L. C. Gupta, C. Godart, B. D. Padalia and R. Vijayaraghavan, Phys. Rev. Lett. **72**, 274 (1994). Link

[3] T. Siegrist, H. W. Zandbergen, R. J. Cava, J. J. Krajewski and W. F. Peck, Jr., Nature (London) **367**, 254 (1994).

[4] P.C. Canfield, P.L. Gammel, and D.J. Bishop, Phys. Today 51 (10), 40 (1998). Link

[5] C. Detlefs, A. H. M. Z. Islam, T. Gu, A. I. Goldman, C. Stassis, P. C. Canfield, J. P. Hill and T. Vogt, Phys. Rev. B 56, 7843 (1997). Link

[6] C. Song, Z. Islam, L. Lottermoser, A. I. Goldman, P. C. Canfield, C. Detlefs, Phys. Rev. B 60, 6223 (1999). Link

[7] B. K. Cho, P. C. Canfield, L. L. Miller, D. C. Johnston, W. P. Beyermann and A. Yatskar, Phys. Rev. B 52, 3684–3695 (1995). Link

[8] B. K. Cho, P. C. Canfield, and D. C. Johnston, Phys. Rev. B 53, 8499 (1996). Link

[9] B. K. Cho, P. C. Canfield, and D. C. Johnston, Phys. Rev. Lett. **77**, 163 (1996). Link

[10] M. E. Fisher, Philos. Mag. 7, 173.1 (1962).

[11] Jens Jensen, Allan R. Mackintosh, Rare Earth Magnetism, Section 5.6.

[12] Jens Jensen, Phys. Rev. B 65, 140514(R) (2002) Link

[13] Jens Jensen, Private Communication

ACKNOWLEDGMENTS

I would like to express my deepest appreciation to my major professor Dr. Paul Canfield for his broad understanding, helpful guidance, friendly discussion and generous support for the past several years. I would also like to express my thanks to Mrs. Canfield for the delicious meals at thanksgiving parties and the wonderful gift for my wedding.

I wish to express my thanks to Dr. Joerg Schmalian for many long and valuable discussions. His profound knowledge in theoretical physics inspired me to think deeper. I would like to give thanks to Dr. Carsten Detlefs. The discussion with him and the following email communications are the start points of my modeling. I also want to express thanks to Dr. Jens Jensen for his careful calculation for my model. I would like to thank Dr. Beongki Cho for his help on my writings. Special thanks go to Dr. Yuri Janssen for his wonderful and friendly discussion with me.

I wish to express appreciation to many professors and colleagues in our department and Ames Laboratory for their encouragement, help and collaborations, especially Dr. Bruce Harmon, Dr. Douglas Finnemore, Dr. Steven Kawaler, Dr. William McCallum, Dr. Vladimir Kogan and Dr. Matthew Kramer. Addition thanks will go to all of the current and previous members of Canfield research group who worked with me together, Ian Fisher, Cedomir Petrovic, Raquel Ribeiro, Marcos Avila, Yuri Janssen, Sergey Bud'ko, Manuel Angst, Xiyue Miao, Rüdeger Wilke, Emilia Morosan and many others for their warmhearted and friendly help.

I am deeply appreciative to my parents and my little sister for their consistent assistance. I wish to express special appreciation to my wife, Zheng Lu. Without her encouragement and unfailing support, this work would have never been possible.